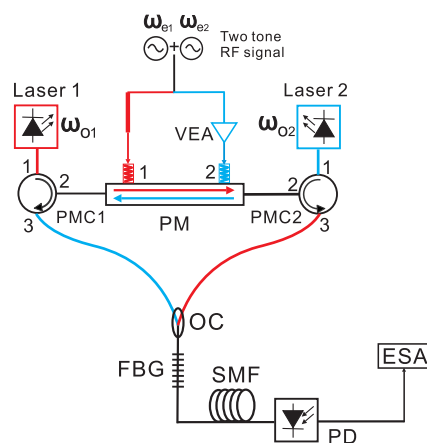


# A Novel High-Linearity Microwave Photonic Link Based on the Strategy of Adding a Compensation Path Using a Bidirectional Phase Modulator

Volume 8, Number 5, October 2016

Tianwei Jiang  
Ruihuan Wu  
Song Yu  
Dongsheng Wang  
Wanyi Gu



DOI: 10.1109/JPHOT.2016.2614500  
1943-0655 © 2016 IEEE

# A Novel High-Linearity Microwave Photonic Link Based on the Strategy of Adding a Compensation Path Using a Bidirectional Phase Modulator

Tianwei Jiang, Ruihuan Wu, Song Yu, Dongsheng Wang,  
and Wanyi Gu

State Key Laboratory of Information Photonics and Optical Communications, Beijing  
University of Posts and Telecommunications, Beijing 100876, China

DOI:10.1109/JPHOT.2016.2614500

1943-0655 © 2016 IEEE. Translations and content mining are permitted for academic research only.  
Personal use is also permitted, but republication/redistribution requires IEEE permission.  
See [http://www.ieee.org/publications\\_standards/publications/rights/index.html](http://www.ieee.org/publications_standards/publications/rights/index.html) for more information.

Manuscript received September 23, 2016; accepted September 26, 2016. Date of publication September 29, 2016; date of current version October 19, 2016. This work was supported in part by the National Basic Research Program of China (973 Program) under Grant 2012CB315605 and Grant 2014CB340102; in part by the National Natural Science Foundation under Grant 61531003, Grant 61427813, and Grant 61271193; in part by China Postdoctoral Science Foundation under Grant 2015M570056; and in part by the Fund of State Key Laboratory of Information Photonics and Optical Communications (Beijing University of Posts and Telecommunications), China. Corresponding author: S. Yu (e-mail: yusong@bupt.edu.cn).

**Abstract:** A novel phase-modulation direct-demodulation microwave photonic link for improving the spurious-free dynamic range (SFDR) is proposed and experimentally demonstrated. In the proposed system, two different C-band optical wavelengths are modulated by a phase modulator in opposite directions. After combining the wavelengths, a fiber Bragg grating (FBG) is used to remove the optical spectrum between the two wavelengths. Because of the natural and wideband  $\pi$  phase difference between the up and low optical sidebands after the phase modulation, third-order intermodulation distortion (IMD3) can be counteracted by subtly designing the optical power and modulation depth relationships between the two wavelengths. The experimental results show that IMD3 is reduced by 28.6 dB, achieving an SFDR improvement of 20 dB compared to a traditional single sideband phase-modulation microwave photonic link.

**Index Terms:** Microwave photonics, microwave photonics signal processing, tunable filter.

## 1. Introduction

Microwave photonic links (MPLs) offering low loss, larger bandwidth, and electro-magnetic interference (EMI) immunity are intensively required for a number of applications such as radars, wireless communications, phased array antennas, and warfare systems [1]. To serve these applications, modern MPLs should have high linearity which is a characteristic that is usually defined as the spurious free dynamic range (SFDR). In the past decades, many linearity strategies have been proposed to improve the SFDR, such as digital post compensation [2], digital pre-distortion [3], optical spectrum processing [4], [11], and the addition of a compensation path [5]–[8]. Among them, digital based methods are limited by the quantization noise which are produced in the process of analog-to-digital conversion. The optical spectrum processing method is limited by the frequency resolution of the spatial light modulator (SLM) [4] or waveshaper [11]. Adding a compensation path

with opposite nonlinearity in the intensity modulation (IM) link is a practical strategy to realize a large SFDR and has been studied by both academic and industrial groups since 1993. This strategy involves the addition of an IM link with opposite bias point, lower optical power and high modulation depth is added to the traditional IM link. In this manner, third-order intermodulation distortion (IMD3) can be counteracted, and hence, SFDR is further improved. Alternatively, the phase modulator has recently attracted increasing attentions because of the following inherent advantages compared to a traditional intensity modulator: 1) It has a high modulation linearity, and 2) no biasing is required for its operation. The phase modulated signal should be converted into an intensity modulated signal for optical-to-electrical conversion. Nonlinearity in the phase modulation system arises from the nonlinearity of PM-to-IM (PM-IM) conversion, such as coherent detection [14], chromatic dispersion fiber (CDF) [15], Mach-Zehnder interferometer (MZI) [16], [17], stimulated Brillouin scattering (SBS) [18], or fiber Bragg grating (FBG) [19].

Haas *et al.* combined the strategy of adding a compensation path with a phase modulator to achieve linearization [17]. However, there are three disadvantages of this method. First, the PM-IM process is achieved by an MZI which is essentially a narrow band device that further limits operation bandwidth of the entire system. Second,  $\pi$  phase difference between the paths is achieved by a 180-degree electrical hybrid coupler. Limited by the phase deviation in this device, it is difficult to ensure the phase accuracy over all of the operational frequencies. Finally, the linearization process requires a sacrifice in gain because the modulation depth ratio is a constant value of 1/3. The gain was reduced by more than 10 dB, mainly because of the increasing of  $V_{\pi}$ .

In this paper, we present a novel SFDR improvement method for a phase-modulation based microwave photonic link based on the strategy of adding a compensation path. Two lightwave beams at different wavelengths are injected into a traveling-wave phase modulator in opposite directions. Because of the velocity mismatch phenomena [21], [22], a lightwave propagating in the positive direction is only modulated by the first electric port; whereas the lightwave propagating in the negative direction is only modulated by the second electric port. The two modulated wavelengths are then combined and pass through an FBG that operates between the two wavelengths. As a result, the up sidebands of a lightwave and down sidebands of another lightwave are filtered out. The remaining optical sidebands of the wavelengths will generate two electrical signals with natural and accurate  $\pi$  phase differences between them. Thus, IMD3 can be counteracted by adjusting the optical power ratio and the modulation depth of the two lightwaves. Because all the optical sidebands are operated in the flat response region of the FBG, the proposed system is a broadband system. Further, SFDR can be improved with only a slight sacrifice in gain. Without specific optical carrier suppression, our SFDR improvement method is not sensitive to wavelength fluctuation. Experimental results demonstrate that IMD3 can be suppressed by 28.6 dB. Compared to the traditional single sideband phase modulation system, the SFDR is improved by over 20 dB and achieves a value of 119.08 dB/Hz<sup>4/5</sup>, while the gain is only reduced by 1.05 dB. Using a high power laser and low relative intensity noise (RIN), an SFDR of 131.88 dB/Hz<sup>4/5</sup> is achieved.

## 2. Topology and principle of operation

Fig. 1(a) shows a conceptual diagram of our proposed microwave photonic link with improved dynamic range. Laser 1 offers a polarization maintain continuous lightwave (lightwave 1) at an angular frequency of  $\omega_{O1}$  that is injected into port 1 of a polarization maintaining circulator (PMC 1). Next, lightwave 1 is modulated by the microwave signal at the first port of a traveling-wave phase modulator (PM). In addition, laser 2 offers another polarization maintained continuous lightwave (lightwave 2) at an angular frequency of  $\omega_{O2}$ . Lightwave 2 is also injected into port 1 of another polarization maintain circulator (PMC 2). At the output of port 2 of PMC 2, lightwave 2 is modulated in the same PM at the second electric port. Because of velocity mismatch phenomena, lightwave 1 and lightwave 2 can be modulated independently. Different from lightwave 1, lightwave 2 provides a lower optical power but is modulated by a larger microwave signal. In other words, lightwave 1 has a large optical power but a lower modulation depth, whereas while the lightwave 2 has a smaller optical power but a larger modulation depth. The two modulated lightwaves are combined

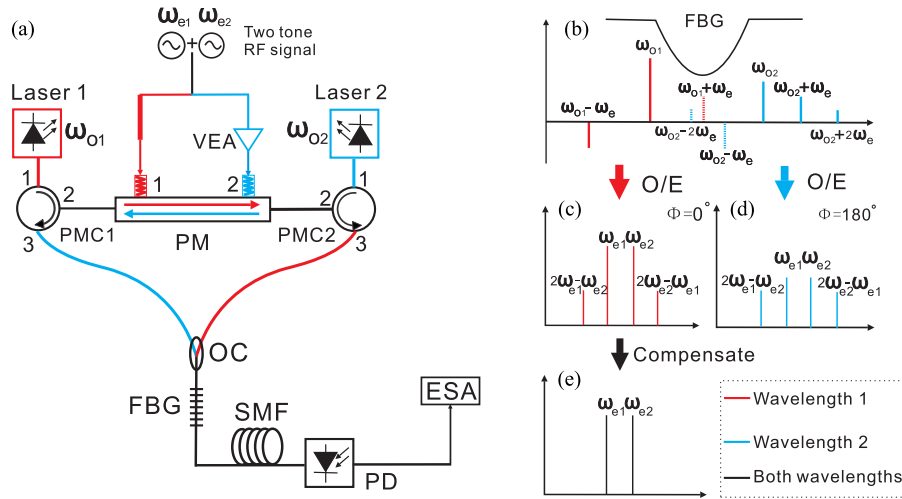


Fig. 1. (a) Diagram of the bidirectional phase-modulated microwave photonic link. ESA: electronic spectrum analyzer. VEA: variable electrical amplifier; SMF: single mode fiber. (b) Optical spectrum of the modulated wavelengths. (c) Detected electrical spectrum from wavelength 1, where  $\Phi$  is the phase of the detected microwave signal. (d) Detected electrical spectrum from wavelength 2. (e) Electrical spectrum when both wavelengths are added.

by an optical coupler (OC) before passing through a fiber Bragg grating (FBG). Fig. 1(b) illustrates the optical spectrum after passing the FBG. By adjusting the center frequency of the FBG, the up sidebands of lightwave 1 and the down sidebands of lightwave 2, which are represented by dotted lines in Fig. 1(b), are filtered out. Next, the remaining optical spectrum is injected into a photodetector (PD). Because the wavelength detuning is larger than the bandwidth of the PD, the optical carrier of each lightwave beats with its own respective sidebands, respectively. If the two-tone microwave signal is used, the detected signals from each lightwave can be illustrated in Fig. 1(c) and Fig. 1(d). We find that detected signals of lightwave 1 stem from the down sidebands; in contrast, the detected signals of  $\omega_{o2}$  stem from up sidebands. Because of the opposite polarity of the  $\pm 1$ st order phase modulated sidebands, a natural and wideband  $\pi$  phase difference is achieved between the two detected microwave signals. By adjusting the optical power and the modulation depth of lightwave 2, we can make the third-order intermodulation distortion (IMD3) from lightwave 2 with equal power but opposite polarity toward IMD3 from lightwave 1. Moreover, the fundamental frequency component from lightwave 2 is significantly lower than that from lightwave 1. Thus, we counteract IMD3 with only a small sacrifice of the gain, as shown in Fig. 1(e) shows. Hence, the spurious free dynamic range (SFDR) can be improved using the proposed approach.

Mathematically, this processing can be expressed by the following equations for the optical fields of both lightwaves at the output of the FBG:

$$u_1(t) = \sqrt{P_1} e^{j\omega_{o1}t} \sum_{l \leq 0} J_l(\beta_1) e^{j l \omega_{e1}t} \quad (1)$$

$$u_2(t) = \sqrt{P_2} e^{j\omega_{o2}t} \sum_{l \geq 0} J_l(\beta_2) e^{j l \omega_{e1}t} \quad (2)$$

where  $P_1$  and  $P_2$  represent the optical powers of lightwave 1 and lightwave 2, respectively.  $\beta_1$  is the modulation depth of lightwave 1;  $\beta_2$  is the modulation depth of lightwave 2; and  $\omega_{e1}$  represents the angular frequency of microwave signal. Because of the incoherent relationship of the two lightwaves, their detected electric fields are generated individually. After the addition of the electric fields in the PD, the photocurrent will be

$$i(t) = I \cos(\omega_{e1}t) \quad (3)$$

where the amplitude of photocurrent  $I$  is defined as

$$I = 2R \left[ P_1 \sum_{l \geq 0} J_l(\beta_1) J_{l+1}(\beta_1) - P_2 \sum_{l \geq 0} J_l(\beta_2) J_{l+1}(\beta_2) \right]. \quad (4)$$

Considering  $\beta_2 = a\beta_1$  and  $P_2 = bP_1$ ,  $a$  is the amplifier factor of VEA, and  $b$  is optical power ratio of the lightwaves. Taylor expansion on (4) to third order in  $\beta_1$  yields

$$I = 2RP_1 \left[ (1 - ab)\beta_1 - \frac{1}{4}(1 - a^3b)\beta_1^3 + \sigma(\beta_1)^5 \right]. \quad (5)$$

From (5), the distortion presented in the photocurrent at microwave frequencies is found to be proportional to  $\beta_1^3$ . The distortion can be eliminated by appropriately choice of the parameters  $a$  and  $b$ , leading to the following linearization condition

$$a^3b = 1. \quad (6)$$

Although the solution for  $a$  and  $b$  is not unique, we also should maximize the component proportional to  $\beta_1$  in (5) that represents the gain of the link. From (5) and (6), we find that large  $a$  and small  $b$  can cancel the distortion components with less gain sacrifice. For example, with the condition of  $a = \sqrt{10}$ ;  $b = (10\sqrt{10})^{-1}$ , the component proportional to  $\beta_1$  will be 0.9. In other words, with an optical power difference of 15 dB and a 5 dB VEA induced electric voltage amplification, the distortion can be eliminated with only a 0.915 dB sacrifice in gain. If both a larger value of  $a$  and smaller value of  $b$  is used, sacrifice in gain can be even lower.

Furthermore, we considered the chromatic dispersion that occurs as the optical signal propagate in the fiber link and induces periodic power fading. As is known, the detected signal from lightwave 2 is much smaller compared to that from lightwave 1; this small signal ultimately influences the fundamental components. In other words, because our proposed link is an approximate single sideband modulation link, it can also combat chromatic dispersion induced power fading. Mathematically, the amplitude of the microwave photocurrent can be shown to be

$$I = RP_1 \left\{ [(1 - ab)e^{jk} + jab \cos(k)] \beta_1 + \frac{1}{4}a^3b \sin^3(k)\beta_1^3 \right\} \quad (7)$$

where  $k = \frac{c\pi L D}{\omega_0^2} \omega_{e1}^2$ ,  $L$  is the fiber length,  $D$  is the chromatic dispersion of the fiber, and  $\omega_0$  is the optical angular frequency. From (7), a small  $ab$  will only induce a small amplitude fluctuation caused by chromatic dispersion. As discussed above, the power fluctuation range should be only 0.91 dB in power with the condition of  $ab = 0.1$ . Thus, our system can overcome power fading caused by chromatic dispersion. In addition, we find that the appearance of the third term and its periodic variation due to chromatic dispersion. It will further cause the SFDR performance to vary periodically. We can calculate that the minimum SFDR will only be 1.3 dB lower than that of the traditional single sideband (SSB) method.

Considering the operational bandwidth, the minimum acceptable RF frequency is determined by the falling edge width of the FBG. The maximum acceptable RF frequency is limited by half the bandwidth of the FBG. As is known, it is easy to manufacture a wideband FBG. Thus, the maximum RF frequency can be up to the THz range, limited only by the bandwidth of the photodetector.

### 3. Experimental results

To verify the proposed method, a proof-of-concept experiment based on the schematic in Fig. 1(a) is performed. A CW polarization-maintaining lightwave (lightwave 1) at 1550.43 nm ( $\omega_{01}$ ) with a power of 15 dBm is provided by a tunable laser (Southern Photonics, TLS150D). Lightwave 1 is then sent to port 1 of PMC 1 (General Photonics) and is outputted from port 2 of PMC 1. Port 2 of PMC 1 is connected to a phase modulator (EOspace,  $V_\pi = 4.3V @ 16$  GHz) with two electric ports (external termination option). Because all of the devices are polarization-maintaining devices, the

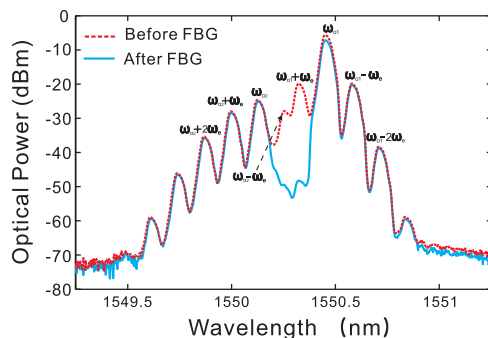


Fig. 2. Modulated optical spectrum before and after the FBG. The dashed line represents the optical spectrum before the FBG; the solid line represents the optical spectrum after the FBG.

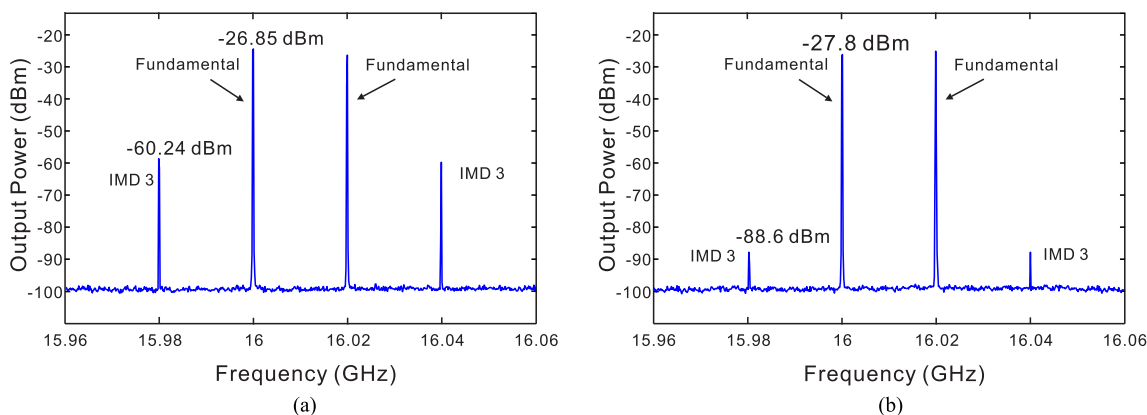


Fig. 3. Two tone test of the PML system using our linearization method. The input power is  $-1$  dBm. The resolution bandwidth is set to be 1 MHz. (a) Traditional SSB system without linearization and (b) our linearization system.

modulation efficiency can be retained. A two-tone microwave signal at frequencies of 16 GHz and 16.02 GHz from two microwave sources (Agilent, E8267D and E8257D, respectively) is divided into two parts. The isolation of microwave power divider is measured to be 25 dB. One part modulates lightwave 1 at port 1 of the PM. Another external cavity laser (Emcore) generates lightwave 2 at 1550.1 nm ( $\omega_{O2}$ ) with a power of 0 dBm ( $b = (10\sqrt{10})^{-1}$ ). The output from port 2 of PMC 2 (General Photonics), lightwave 2 is injected into the same PM in the opposite direction. At port 2 of the PM, the other part of the two-tone signal is amplified by 10 dB in power after passing an electric amplifier modulates lightwave 2. After adjusting the VEA and setting  $a = \sqrt{10}$ , lightwave 1 and lightwave 2 are returned to port 2 and output from port 3 of PMC 2 and PMC 1, respectively. An optical delay line (OZ Photonics) is used to match the transport length between the paths. An optical coupler (OC) combines the lightwaves. An FBG (AOS) with a center wavelength of 1550.29 nm and bandwidth of 42 GHz filters out the optical spectrum between the wavelengths. The dotted line in Fig. 2 shows the modulated optical spectrum measured by optical spectrum analyzer (YOKOGAWA, AQ6370B). We find that  $\omega_{O1}$  has a high optical carrier power and a low modulation sideband power compared to  $\omega_{O2}$ . After filtering, the up sidebands of lightwave 1 and the down sidebands of lightwave 2 are suppressed. The other remaining optical spectrum passes through the transmission port, as indicated by the solid line in Fig. 2. The output optical power which is measured to be 3.4 dBm is received by a PD with a responsivity of 0.9 A/W (Picometrix, P-18A). An electrical spectrum analyzer (Rohde-Schwarz, FSV 30) is used to analyze the signal.

To investigate the suppression of IMD3, we measure the traditional SSB-PM link by disconnecting wavelength 2 in Fig. 1(a). The optical power measured before PD is 3 dBm. The distortion components can be observed via a non-linear PM-IM transfer function. In Fig. 3(a), the fundamen-



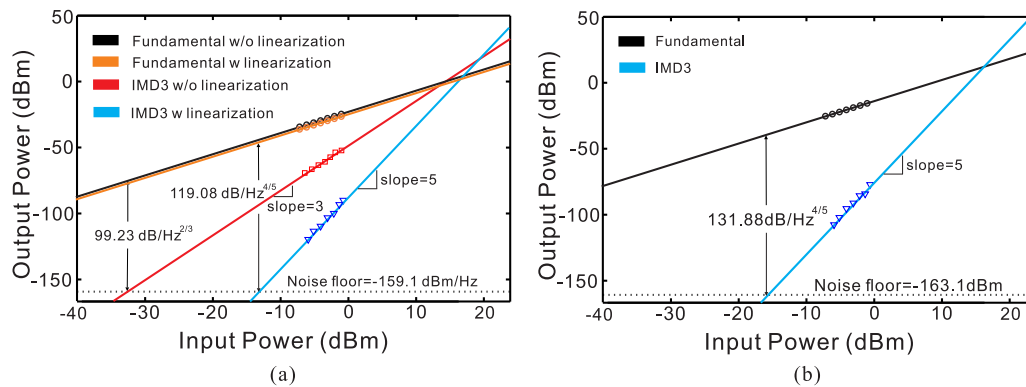


Fig. 4. Fundamental and intermodulation signal as a function of the RF input power for the different systems. The black curve is the fundamental power for the traditional SSB system, the orange curve is the fundamental power for our system, the red curve is the IMD3 for the traditional SSB system, and the blue curve is the IMD3 for our system. (a) Using commercial laser. (b) Using a high power and low RIN laser.

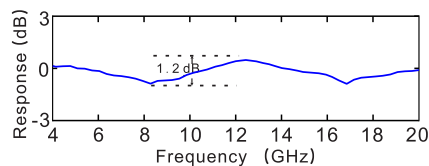


Fig. 5. Response of 41 km SMF links normalized to the traditional chromatic dispersion overcoming the SSB system.

tal frequency components have a power level of  $-26.85$  dBm, the IMD3 power is  $-60.24$  dBm. As shown in Fig. 3(b), IMD3 is significantly suppressed to  $-88.6$  dBm after adding wavelength 2, whereas the fundamental frequency signal power is slightly reduced to  $-27.8$  dBm. This observation is in good agreement with theoretical analysis above.

We also measure the SFDR of our high linear link for a traditional SSB-PML, as shown in Fig. 4(a). The optical power of 3.4 dBm result in the noise floor being  $-159.1$  dBm/Hz; this noise floor includes both shot noise and thermal noise. IMD3 in the traditional SSB-PML is limited by the term proportional to  $\beta_1^3$  in (5). As a result, the slope is 3. After linearization, the term proportional to  $\beta_1^3$  is eliminated. The term proportional to  $\beta_1^5$  dominates the IMD3 and further change the slope to 5. Ultimately, the SFDR is improved from  $99.23$  dB/Hz $^{2/3}$  to  $119.08$  dB/Hz $^{4/5}$ . To obtain a larger SFDR, a laser (Emcore 1782B) with 20 dBm power and  $-168$  dBc/Hz relative intensity noise is used as laser 1. Phase modulator with low loss option (insert loss is 1.8 dB) replaces the standard modulator. The resulting experimental SFDR performance is shown in Fig. 4(b). We find that the gain of the system is improved and the noise floor is reduced to  $-163$  dBm. Ultimately, an SFDR of  $131.88$  dB/Hz $^{4/5}$  is achieved.

We measure the frequency response from 4 GHz to 20 GHz by vector network analyzer (Agilent, 8722ES) after adding a 41-km single-mode fiber (SMF) between the FBG and the PD. Fig. 5 shows the frequency response result. The periodic amplitude fluctuation is found to be due to chromatic dispersion. However, the fluctuation range is just only 1.2 dB from 4 to 20 GHz. Thus, the response can be nearly considered to be a flat response. The decreased effect of the FBG will decrease the gain of the system when the frequency is below 4 GHz. If the gain decrease value for both of the paths is the same, the IMD3s can also be counteracted. However, the SFDR will be reduced because of the gain reduction.

## 4. Conclusion

In conclusion, a novel dynamic range improvement method for a phase-modulation based microwave photonic link (PM-MPL) was proposed and experimentally demonstrated. In the proposed link, we use two different wavelengths modulated with different modulation depths in opposite directions. The modulated signal is then combined and filtered by the FBG. By adjusting the optical powers of the two wavelengths to a proper ratio, a third-order intermodulation distortion (IMD3) is counteracted, thereby further improving the SFDR. Thus, a high dynamic range PM-MPL with little sacrifice in gain was implemented. The experimental results show that the IMD3 is reduced by 28.6 dB, achieving a spurious-free dynamic range (SFDR) improvement of approximately 20 dB compared to the traditional single sideband phase-modulation based microwave photonic link. The gain is only reduced by 1.05 dB. Moreover, our high dynamic range PM-MPL can also combat the periodic power reduction caused by chromatic dispersion.

## References

- [1] J. Capmany and D. Novak, "Microwave photonics combines two worlds," *Nature Photon.*, vol. 1, no. 6, pp. 319–330, 2007.
- [2] Y. Cui *et al.*, "Enhanced spurious-free dynamic range in intensity-modulated analog photonic link using digital postprocessing," *IEEE Photon. J.*, vol. 6, no. 2, pp. 1–8, Apr. 2014.
- [3] A. Agarwal, T. Banwell, P. Toliver, and T. K. Woodward, "Predistortion compensation of nonlinearities in channelized RF photonic links using a dual-port optical modulator," *IEEE Photon. Technol. Lett.*, vol. 23, no. 1, pp. 24–26, Jan. 2011.
- [4] G. Zhang, X. Zheng, S. Li, H. Zhang, and B. Zhou, "Postcompensation for nonlinearity of Mach–Zehnder modulator in radio-over-fiber system based on second-order optical sideband processing," *Opt. Lett.*, vol. 37, no. 5, pp. 806–808, 2012.
- [5] J. L. Brooks, G. S. Maurer, and R. A. Becker, "Implementation and evaluation of a dual parallel linearization system for AM-SCM video transmission," *J. Lightw. Technol.*, vol. 11, no. 1, pp. 34–41, Jan. 1993.
- [6] K. Adil and J. Devenport, "Low noise figure microwave photonic link," in *Proc. IEEE/MTT-S Int. Microw. Symp.*, 2007, pp. 1519–1522.
- [7] L. Xianghua, Y. Chun, Z. Zhenghua, and C. Yuhua, "Dynamic range improvement of IM-DD optical link using dual-wavelength dual-parallel modulation," *J. Opt. Soc. Korea*, vol. 18, no. 4, pp. 330–334, 2014.
- [8] P. Joaquin and R. Llorente, "On the performance of a linearized dual parallel Mach–Zehnder electro-optic modulator," *Opt. Commun.*, vol. 318, pp. 212–215, 2014.
- [9] J. Li, Y.-C. Zhang, S. Yu, T. Jiang, Q. Xie, and W. Gu, "Third-order intermodulation distortion elimination of microwave photonics link based on integrated dual-drive dual-parallel Mach–Zehnder modulator," *Opt. Lett.*, vol. 38, no. 21, pp. 4285–4287, 2013.
- [10] D. Marpaung, C. Roeloffzen, A. Leinse, and M. Hoekman, "A photonic chip based frequency discriminator for a high performance microwave photonic link," *Opt. Exp.*, vol. 18, no. 26, pp. 27359–27370, 2010.
- [11] P. Li *et al.*, "Improvement of linearity in phase-modulated analog photonic link," *Opt. Lett.*, vol. 38, no. 14, pp. 2391–2393, 2013.
- [12] W. Li and J. Yao, "Dynamic range improvement of a microwave photonic link based on bi-directional use of a polarization modulator in a Sagnac loop," *Opt. Exp.*, vol. 21, no. 13, pp. 15692–15697, 2013.
- [13] W. Li, L. X. Wang, and N. H. Zhu, "Highly linear microwave photonic link using a polarization modulator in a sagnac loop" *IEEE Photon. Technol. Lett.*, vol. 26, no. 1, pp. 89–92, Jan. 2014.
- [14] T. R. Clark and M. L. Dennis, "Coherent optical phase-modulation link" *IEEE Photon. Technol. Lett.*, vol. 19, no. 16, pp. 1206–1208, 2007.
- [15] H. Chi, X. Zou, and J. Yao, "Analytical models for phase-modulation-based microwave photonic systems with phase modulation to intensity modulation conversion using a dispersive device" *J. Lightw. Technol.*, vol. 27, no. 5, pp. 511–521, Mar. 2009.
- [16] S. Pan and J. Yao, "Switchable UWB pulse generation using a phase modulator and a reconfigurable asymmetric Mach–Zehnder interferometer," *Opt. Lett.*, vol. 34, no. 2, pp. 160–162, 2009.
- [17] B. M. Haas, V. J. Urlick, J. D. McKinney, and T. E. Murphy, "Dual-wavelength linearization of optically phase-modulated analog microwave signals," *J. Lightw. Technol.*, vol. 26, no. 15, pp. 2748–2753, Aug. 2008.
- [18] X. S. Yao, "Phase-to-amplitude modulation conversion using Brillouin selective sideband amplification," *IEEE Photon. Technol. Lett.*, vol. 10, no. 2, pp. 264–266, Feb. 1998.
- [19] V. R. Pagán, B. M. Haas, and T. E. Murphy, "Linearized electrooptic microwave downconversion using phase modulation and optical filtering" *Opt. Exp.*, vol. 19, pp. 883–895, 2011.
- [20] D. Lam, A. M. Fard, B. Buckley, and B. Jalali, "Digital broadband linearization of optical links," *Opt. Lett.*, vol. 38, no. 4, pp. 446–448, 2013.
- [21] W. R. Leeb, A. L. Scholtz, and E. Bonek, "Measurement of velocity mismatch in traveling-wave electrooptic modulators," *IEEE J. Quantum Electron.*, vol. QE-18, no. 1, pp. 14–16, Jan. 1982.
- [22] T. Jiang, S. Yu, Q. Xie, J. Li, and W. Gu, "Photonic downconversion based on optical carrier bidirectional reusing in a phase modulator," *Opt. Lett.*, vol. 39, no. 17, pp. 4990–4993, 2014.